ON THE TRANSITION FROM RIDGED WAVEGUIDE TO MICROSTRIP

W. Menzel*, A. Klaassen

ABSTRACT

In conjunction with the transition from waveguide to microstrip via a rigded waveguide structure, two problems are investigated. The first one concerns the impedance of the ridged structure including a dielectric layer on the bottom of the waveguide, the second one the field discontinuity when an unloaded ridged waveguide with wide ridge is connected to a high ϵ_r microstrip of the same impedance but much smaller width.

I. Introduction

For the RF evaluation of mm-wave MMICs, broadband, well matched and reproducible transitions from a waveguide measurement system to the MMIC chip - in most cases in microstrip technique - is of great importance /1/. Typical transitions of this kind are shown in Fig. 1. The probe-type transition is a relative simple arrangement and is often used in system applications; for a good match it is, however, mostly narrowband. The waveguide-finline-microstrip transition is good, but relatively lossy, and problems may occur with resonances if it is used for broadband operation. Therefore, the transition via a ridged waveguide is employed very often.

With this type of transition two questions arise which are dealt with in this contribution. The first one concerns the impedance of the ridge structure at the end of the waveguide which has to match to that of the adjacent microstrip. The basic field configurations of both structures are similar; the impedance of the ridge structure however may be influenced by the "thick" metallization, speaking in microstrip terms.

The second question arises from the fact that in an unloaded ridged waveguide, i.e. no dielectric is used there, the ridge width may be much larger than the line width of a microstrip for a given impedance. This does not lead to an impedance but to a field configuration discontinuity.

II. Impedance of the ridged waveguide structure

A cross-section of ridged waveguide with typical dimensional relations is shown in Fig. 2. A dielectric layer is introduced at the bottom of the waveguide giving an improved field match to a microstrip (/1/).

The electromagnetic field mainly is concentrated in the area under the ridge. For the calculation of this structure, this fact gives the chance to reduce the waveguide region under investigation by introducing a magnetic wall as shown by the broken lines in Fig. 2. In an analysis of a complete waveguide cross-section of this kind, the computational effort would be much higher, as - in contrast to /2/ - the number of mode terms could not be reduced to only a few modes representing the field under the ridge or the current on the bottom of the ridge without inversion of a much larger matrix.

TELEFUNKEN SYSTEMTECHNIK, PO Box 17 30, D-7900 Ulm, FRG
* since Aug. 1, 1989: University of Ulm, Electr. Eng. Dptm., Microwave Technique, Oberer Eselsberg, D-7900 Ulm, FRG.

The analized structure (for even modes only!) is shown in Fig. 3. A standard procedure using LSM and LSE modes /2/, together with a mode matching procedure was used to determine the phase velocity employing the following potentials in the two regions (Fig. 3):

Region I:
$$\psi_{tm}^{I(h)} = A_m \cos\left(\frac{m\pi}{a}x\right) \cos\left(k_{ym}^{I}\, y\right) \quad , \ m \geq 0$$

$$\psi_{tn}^{I(e)} = B_n \sin\left(\frac{n\pi}{a}x\right) \sin\left(k_{yn}^{I}\, y\right) \quad , \ n \geq 1$$

Region II:
$$\psi_{tp}^{II(h)} = C_p \sin\left(\frac{(2p-1)\pi}{2(a-w)}(x-w)\right) \cos\left(k_{yp}^{II}(y-d-h)\right) \quad , \ p \geq 1$$

$$\psi_{tq}^{II(e)} = D_q \cos\left(\frac{(2q-1)\pi}{2(a-w)}(x-w)\right) \sin\left(k_{yq}^{II}(y-d-h)\right) \quad , \ q \geq 1$$

with
$$\gamma^2 = \left(\frac{m\pi}{a}\right)^2 + k_{ym}^{I\,2} - k_0^2\, \varepsilon_r$$

$$= \left(\frac{2p-1}{2(a-w)}\pi\right)^2 + k_{yp}^{II\,2} - k_0^2$$

From these potentials, the E and H field components can be derived in the following way:

$$\vec{E}^{i} = \frac{1}{j\omega\varepsilon_0\varepsilon_r^{i}} \left\{ \frac{\partial^2}{\partial x \partial y} , -\gamma^2 - \frac{\partial^2}{\partial x^2} , -\gamma \frac{\partial}{\partial y} \right\} \psi_t^{i(h)} e^{-\gamma z}$$
$$+ \left\{ \gamma \ , \ 0 \ , \ \frac{\partial}{\partial x} \right\} \psi_t^{i(e)} e^{-\gamma z}$$

$$\vec{H}^{i} = \left\{ \gamma \ , \ 0 \ , \ \frac{\partial}{\partial x} \right\} \psi_t^{i(h)} e^{-\gamma z}$$
$$+ \frac{1}{j\omega\mu_0} \left\{ -\frac{\partial^2}{\partial x \partial y} , \gamma^2 + \frac{\partial^2}{\partial x^2} , \gamma \frac{\partial}{\partial y} \right\} \psi_t^{i(e)} e^{-\gamma z}$$

The mode matching procedure leads to a homogeneous set of equations with real coefficients. The phase velocity of the fundamental mode of the structure is found by determining the first zero of the system determinant. By setting one of the unknowns of the system of equations to 1, for example, the system can be solved for the remaining unknown coefficients, from which electric and magnetic fields can be computed.

For the impedance of this (quasi-TEM in this appoximation!) structure, a definition of voltage integrated in the symmetry plane and current on the bottom of the waveguide was used giving a very simple calculation procedure.

A convergence investigation showed that the number of modes in the two regions should be
$$n \geq \frac{3}{2} \cdot \frac{a}{w}$$

The widths a in Fig. 3 should be 4 times the substrate thickness for w not too large.

A typical result for a waveguide with an alumina substrate on the bottom (as used in /1/) is given in Fig. 4.

Differences compared to a corresponding microstrip occur as well in phase velocity or in effective dielectric constant as in line impedance as shown in this figure. These calculations show that an improvement in the match of this transition is possible by properly adjusting the impedances of ridged waveguide and microstrip line.

III. Impedance match of a transition without dielectric in the ridged waveguide

A somewhat different configuration arises if no dielectric layer is placed in the ridged waveguide. To maintain impedance match, the widths of the ridge and of the microstrip line differ considerably, in the case of a microstrip line on GaAs by a factor of approximately 10 (/4/). Again, the procedure described in section II can be used to calculate the impedance of the ridged waveguide. Due to the great difference in width, the field configurations of the two transmission line structures do not fit directly. To estimate the effect of this field discontinuity, a computer program for step discontinuities in microstrip lines (/5/) was modified to allow different dielectric materials in the two lines (Fig. 5). For a microstrip impedance of 75 Ω (2w = 0,056 mm), the reflection coefficient of the transition to an unloaded ridged waveguide is plotted in Fig. 6 as a function of ridge width.

A variation of the ridge width shows a minimum reflection coefficient of 0.13 for a ridge width of 0.5 mm (impedance 69 Ω), the minimum however is very flat. A further improvement is possible only by compensating the reactive effects of the discontinuity. These calculations strongly are supported by the results of /4/.

IV. Conclusion

These investigations point out the effects which affect the design of a good broadband transition from waveguide to microstrip, especially the effects of impedance and field discontinuities. Taking these into account, it is possible to build such transitions with a return loss better than 20 dB over a complete waveguide band.

REFERENCES

/1/ Adelseck, B.; et al.: A 35 GHz Monolithic Receiver. Military Microw. Conf. 1988, London, 505-510.

/2/ Schmidt, L.-P.: On the field theoretical calculation of transversal discontinuities in microstrip lines. Doctoral thesis 1979, Aachen. W.-Germany (in German)

/3/ Kirschning, H.; Jansen, R.H.: Accurate model for effective dielectric constant of microstrip with validity up to mm-wave frequencies. Electron. Lett, 18 (1982), 272-273.

/4/ Bogner, W.; Freyer, J.: Microstrip Power Combiner/Divider at 60 GHz on Semiinsulating GaAs. AEÜ, 43 (1989), 187-190.

/5/ Kompa, G.: S-matrix computation of microstrip discontinuities with a planar waveguide model. AEÜ, 1976, 58-64.

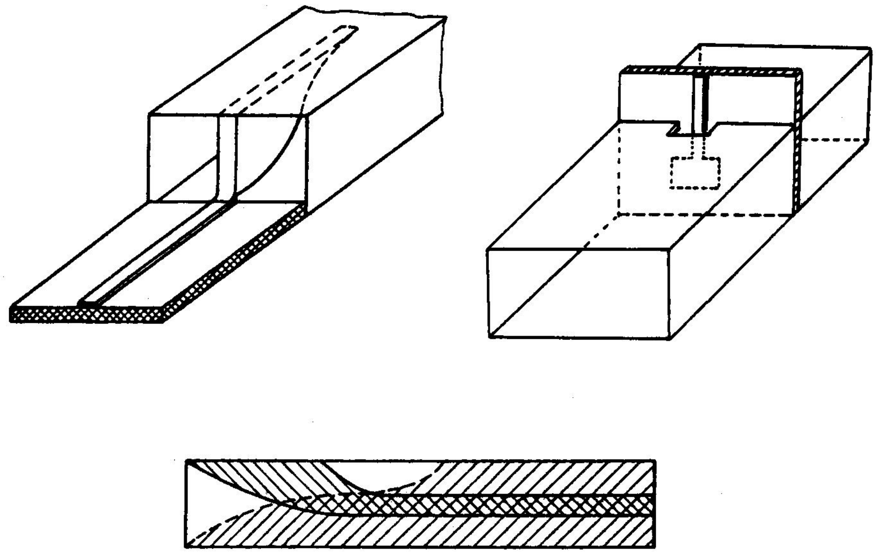

Fig. 1: Transitions from metal waveguide to microstrip

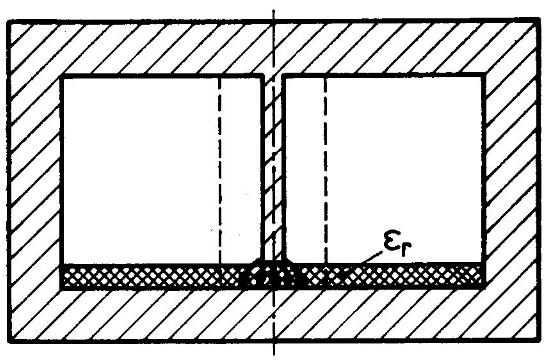

Fig. 2: Cross-section of a typical ridged waveguide structure

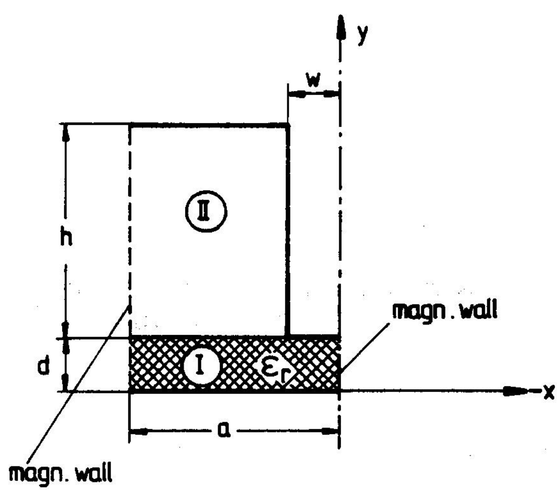

Fig. 3: Reduced size waveguide structure

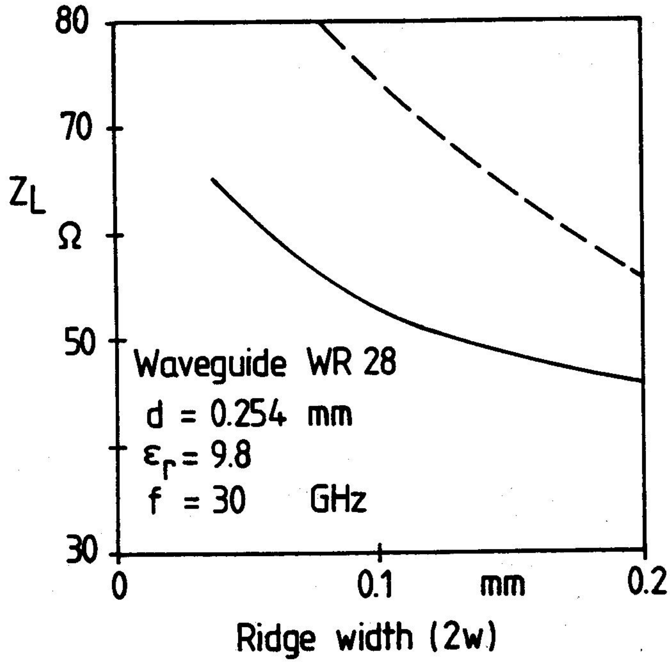

Fig. 4:Characteristic impedance of a loaded ridged waveguide (——) and of an equivalent microstrip line (-----) .

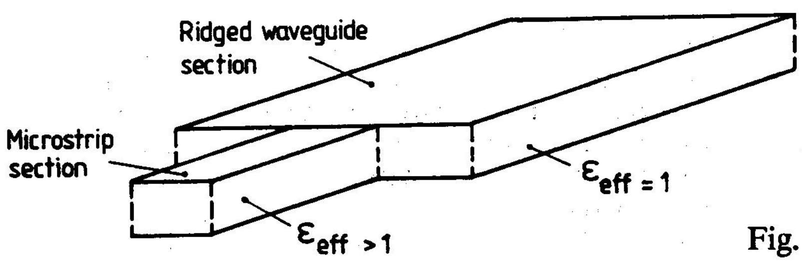

Fig. 5: Step discontinuity

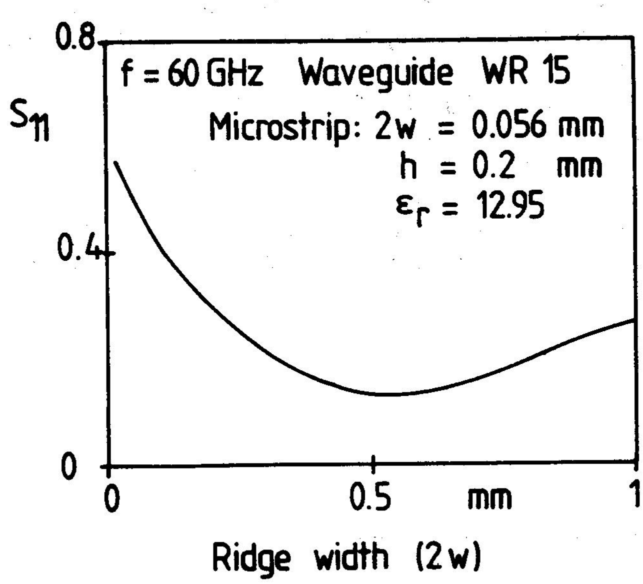

Fig. 6: Reflection coefficient of a transition from microstrip to unloaded ridged waveguide.